sciendo
Austrian Journal of Earth Sciences | Vienna | 2020 | Volume 113/2 | 139 - 154 | DOI: 10.17738/ajes.2020.0009

Polyphase deformation along the South Bohemian Batholith-Moldanubian nappes boundary – The Freyenstein Fault System (Bohemian Massif/Austria)

Gerit E. U. GRIESMEIER[1]*, Christoph IGLSEDER[1], Ralf SCHUSTER[1] & Konstantin PETRAKAKIS[2]
[1)]Geological Survey of Austria, Neulinggasse 38, 1030 Vienna, Austria;
[2)]Department of Geodynamics and Sedimentology, University of Vienna, Althanstrasse 14, 1090 Vienna, Austria;
*) Corresponding author, gerit.griesmeier@geologie.ac.at

KEYWORDS shear zone, fault, Moldanubian Superunit, petrology, structural geology, Rb-Sr geochronology

Abstract
This work describes the Freyenstein Fault System, which extends over 45 km in the southeastern part of the Bohemian Massif (Lower Austria). It represents a ductile shear zone overprinted by a brittle fault located at the eastern edge of the South Bohemian Batholith towards the Moldanubian nappes. It affects Weinsberg- and a more "fine-grained" granite, interlayered aplitic granite and pegmatite dikes as well as paragneiss of the Ostrong Nappe System. The ductile shear zone is represented by approximately 500 m thick greenschist-facies mylonite dipping about 60° to the southeast. Shear-sense criteria like clast geometries, SCC`-type shear band fabrics as well as abundant microstructures show top to the south/southsouthwest normal shearing with a dextral strike-slip component. Mineral assemblages in mylonitized granitoid consist of pre- to syntectonic muscovite- and biotite-porphyroclasts as well as dynamically recrystallized potassium feldspar, plagioclase and quartz. Dynamic recrystallization of potassium feldspar and the stability of biotite indicate upper greenschist-facies metamorphic conditions during the early phase of deformation. Fluid infiltration at lower greenschist-facies conditions led to local sericitization of feldspar and synmylonitic chloritisation of biotite during a later stage of ductile deformation. Finally, a brittle overprint by a north-south trending, subvertical, sinistral strike-slip fault that shows a normal component is observed. Ductile normal shearing along the Freyenstein Shear Zone is interpreted to have occurred between 320 Ma and c. 300 Ma. This time interval is indicated by literature data on the emplacement of the hostrock and cooling below c. 300°C inferred from two Rb-Sr biotite ages measured on undeformed granites close to the shear zone yielding 309.6 ± 3 Ma and 290.9 ± 2.9 Ma, respectively. Brittle sinistral strike-slip faulting at less than 300°C presumably took place not earlier than 300 Ma. Early ductile shearing along the Freyenstein Fault System may be genetically, but not kinematically linked to the Strudengau Shear Zone, as both acted in an extensional regime during late Variscan orogenic collapse. A relation to other major northeast-southwest trending faults of this part of the Bohemian Massif (e.g. the Vitis-Pribyslav Fault System) is indicated for the phase of brittle sinistral movement.

1 Introduction

In the southern part of the Bohemian Massif, a number of late Carboniferous to early Permian fault systems (FS) related to the Variscan orogenic event are known. Several of these exhibit a polyphase evolution from earlier ductile shear zones, later overprinted or reactivated as brittle strike-slip faults. Beside some specific features discussed below, two dominant fault sets have been identified based on their orientation (Fig. 1): a westnorthwest-eastsoutheast oriented set with dextral offset, including for example the Danube FS and Pfahl FS and a northeast-southwest trending one that exhibits sinistral kinematics, including for example the Rodl-Kaplice FS, Karlstift FS, Vitis-Pribyslav FS or Diendorf-Boscovice FS (Brandmayr et al., 1995).

The tectonic structure here referred to as Freyenstein Fault System (FS) is known since more than 40 years, but was never focus of a structural study. Parts of it were mapped for the first time by Thiele (1976) as well as Fuchs and Matura (1976) in their overview map of the Bohemian Massif. Descriptions of mylonite and fault development are lacking in these early publications, but were described briefly by Fuchs (1984; 2005), Thiele (1969) and Fuchs and Roetzel (1990). Its extent is shown in the geologic map of Upper Austria (Krenmayr et al., 2006). In all mentioned publications, the discussed structure was claimed to be a (sub)vertical, sinistral strike-slip fault.

In this contribution, the Freyenstein FS is described on the basis of the affected country rock, the appearing fault rock and the deformation kinematics. Its time of activity is inferred from literature data on the crystallization of the deformed magmatic rocks and new Rb-Sr biotite ages. Finally, its relation to other shear zones in the southern Bohemian Massif is discussed.

2 Regional geological setting

The southern Bohemian Massif is traditionally subdivided into the Moldanubian and Moravian Superunits, which formed during the Variscan orogenic event (Suess, 1911; Tollmann, 1982; Franke, 2000). The Moldanubian Superunit consists of the Moldanubian nappes, the South and Central Bohemian Batholith as well as the Bavarian Massif (Fig. 1). The Moldanubian nappes are built up by three nappe systems (Linner, 2013), which are characterized by different lithological composition and metamorphic evolution. In the uppermost Gföhl Nappe System, eclogite-facies (Kotková, 2007; Schantl et al., 2019) and partly even ultrahigh-pressure peak metamorphic conditions (Faryad, 2009; Perraki and Faryad, 2014) are described, followed by granulite-facies metamorphic conditions in both the Gföhl and the underlying Drosendorf Nappe Systems (Petrakakis, 1997; Sorger et al., 2020). Within the lowermost Ostrong Nappe System, some eclogite lenses appear in a matrix of monotonous paragneiss, which attained prograde amphibolite-facies conditions, followed by subsequent anatexis (Petrakakis, 1997). $^{40}Ar/^{39}Ar$ muscovite ages indicate cooling below c. 400°C at around 320 Ma in the Ostrong Nappe System (e.g. Zeitlhofer et al., 2013). Geochronological investigations on "weakly-deformed" pegmatite bodies (Ertl et al., 2012) and granitoides of the South Bohemian Batholith (e.g. Klötzli and Parrish, 1996; Klötzli et al., 1999), which intersect the Moldanubian nappes, point to a nappe stacking prior to c. 340 Ma.

In the South Bohemian Batholith, Waldmann (1930) distinguished four different types of plutonic suites: Alkaline magmas, "Kristallgranit" (today´s Weinsberg granite), Mauthausen and Eisgarn granite. Based on geochemical analysis, geochronological data and magmatic features, these granite types were subdivided in more detail later on (e.g. Fuchs and Matura, 1976; Koller et al., 1993; Klötzli et al., 1999; Finger and Schubert, 2015). From c. 338 Ma onward, main plutonic activity started with the intrusion of the Rastenberg granodiorite (Klötzli and Parrish, 1996), followed by diorite bodies between 334 and 332 Ma (Vellmer and Wedepohl, 1994). The widespread Weinsberg granite (WBG) started intruding at c. 330 Ma. However, towards the southwest, it shows decreasing intrusion ages (Friedl, 1997; Gerdes et al., 2003) with the youngest of 322 Ma reported from the Bavarian Massif (Finger et al., 2009). Around 310 Ma, the WBG had already cooled below 450°C (Scharbert et al., 1997). In addition to its widespread I-type chemistry, the WBG exhibits locally S-type signatures (Scharbert, 1987; Finger and von Quadt, 1992).

Two-mica granite with S-type signature, commonly referred to as Eisgarn granite, intruded around 328-325 Ma. It is located in the northern part of the South Bohemian Batholith (Finger and Schubert, 2015). Between 322 and 316 Ma middle- to „fine-grained" granite melts with I-type signatures like the Mauthausen granite intruded the already existing batholith (Gerdes et al., 2003; Rupp et al., 2011). The Freistadt granodiorite forms the youngest pluton with an intrusion age of c. 310-300 Ma (Gerdes et al., 2003).

The Bavarian Massif, located at the southwestern border of the Bohemian Massif, shows an additional metamorphic evolution that is unique to the rest of the Bohemian Massif. Contemporaneously to magma intrusions of the South Bohemian Batholith, the "Bavarian rocks", being already placed at mid-crustal levels, were extensively overprinted at high temperatures by the so called Bavarian event (Finger et al., 2007). This caused widespread migmatization, leucosome segregation and formation of singular bodies of S-type granite intrusions (Rupp et al., 2011 and references therein). The Bavarian event is placed between c. 325-300 Ma with peak metamorphic conditions around 315-312 Ma (Sorger et al., 2018).

During the Late Mississippian (331-323 Ma), the Moldanubian nappes were thrust onto the Moravian Superunit along a major mylonitic shear zone referred to as Moldanubian Thrust (Fig. 1; Suess, 1908; Fritz et al., 1996; Štípská et al., 1999). This thrust is characterized by top to the north/northeast sense of shear with $^{40}Ar/^{39}Ar$ amphibole cooling ages from 342 Ma to 332 Ma (Racek et al., 2017) and muscovite cooling ages from 331 Ma to 325 Ma. Two generations of lamprophyric dikes dissect parts of the Moldanubian and Moravian Superunits. The first generation is "weakly-metamorphosed", trends westnorthwest-eastsoutheast and yields $^{40}Ar/^{39}Ar$ biotite plateau ages around 323 Ma, whereas a second unmetamorphosed group is northnortheast-southsouthwest-trending and yields $^{40}Ar/^{39}Ar$ plateau ages of 315-306 Ma (Neubauer et al., 2003). Additionally, Rb-Sr biotite cooling ages yielding c. 322-311 Ma on "partly-deformed" lamprophyric and porphyric dikes are described in the Strudengau area (Zeitlhofer et al., 2016).

Late Variscan orogenic collapse and plate reorganization in Pennsylvanian to early Permian times (c. 325-290 Ma; Kroner and Romer, 2013) led to the formation of several fault systems cutting through the Moldanubian and Moravian Superunits (Fig. 1). They may be distinguished by their orientation, timing of activity, deformation mechanism and kinematics. Time constraints are often restricted to upper age limits based on crosscutting relations to various granitic bodies with known intrusion ages. However, for some of the shear zones more precise geochronological information is available. A unique structure is the Strudengau Shear Zone (Fig. 1), because of its subhorizontal orientation. It shows top to the northwest sense of shear at greenschist-facies conditions between 323 and 318 Ma (Zeitlhofer et al., 2013). All other fault systems are subvertical and based on their orientation three main groups can be distinguished. The earliest westnorthwest-eastsoutheast trending ones (e.g. Pfahl and Danube FS) show mainly dextral strike-slip kinematics. The Pfahl Shear Zone initiated at metamorphic conditions around 650°C (Brandmayr et al., 1995) between 335 to 330 Ma, as given by intrusion ages of syntectonic palite (Siebel et al., 2005). For the Danube FS, Brandmayr et al. (1995) described greenschist-facies conditions at c. 287 Ma, as inferred by 40Ar/39Ar dating on synkinematically grown muscovite. North(north) east-south(south)west trending structures (e.g. Lhenice

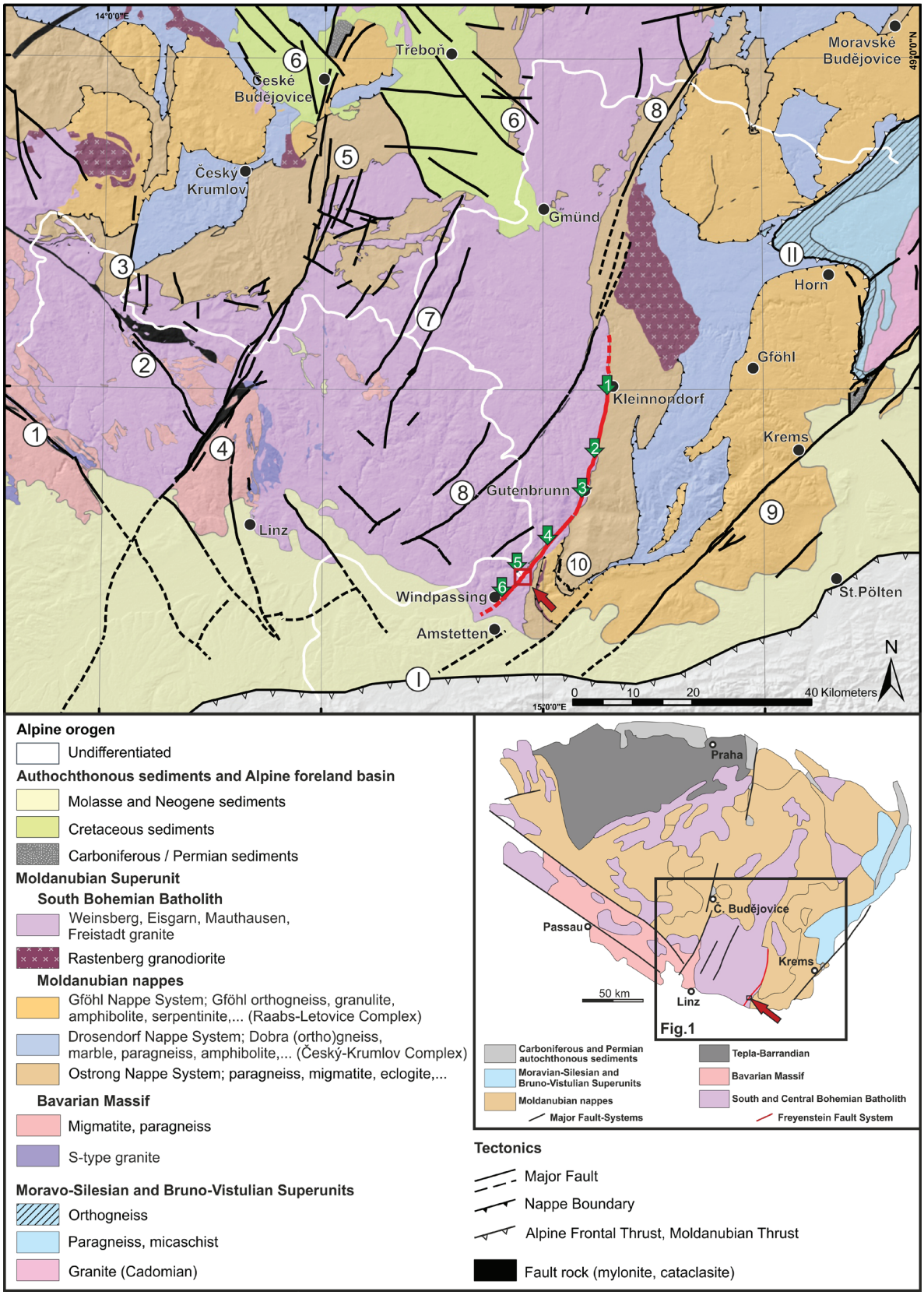

Fig. 1: Geological overview of the southern Bohemian Massif. The Freyenstein Fault System (red line) is located at the southeastern edge of the South Bohemian Batholith. The investigated area along the Danube river (Fig. 2) is marked by red arrow and square. Green arrows with numbers represent additional locations along the FS, which were briefly observed. Numbers are explained in the text (section 3). Localities are given in Table 1 and are named as follows: 1 – GG20003, 2 – GG20004, 3 – GG20001, 4 – GG20006, 5 – PMM14/09, 6 – GG20009. The map is based on Schnabel et al. (2002), Krenmayr et al. (2006) and Cháb et al. (2007). Numbers in white circles indicate the following fault systems (FS): 1 – Danube FS, 2 – Pfahl FS, 3 – Lhenice Graben FS, 4 – Rodl-Kaplice FS, 5 – Kourim-Blanice FS, 6 – Jachymov FS, 7 – Karlstift FS, 8 – Vitis-Pribyslav FS, 9 – Diendorf-Boscovice FS, 10 – Strudengau Shear Zone. I – Alpine Frontal Thrust, II – Moldanubian Thrust. The overview map is based on Wallbrecher et al. (1996), Brandmayr et al. (1999), Büttner (2007), Cháb et al. (2007) as well as Kroner and Romer (2013). Federal boundaries are in white.

Graben, Rodl-Kaplice, Kourim-Blanice, Karlstift, Vitis-Pribyslav and Diendorf-Boskovice FS) record predominantly sinistral strike-slip kinematics. Fault rocks along the Rodl and Karlstift Shear Zones in the west evolved at (upper) greenschist-facies conditions, whereas in the east, dominant brittle deformation is recorded along the Vitis and Diendorf Faults (Wallbrecher et al., 1991; Brandmayr et al., 1995, 1999; Büttner, 2007). These observations reflect decreasing deformation temperatures from west to east.

For the Rodl Shear Zone, the tectonic activity is dated by synkinematically grown muscovite yielding 288-281 Ma (Brandmayr et al., 1995). In contrast, the Pribyslav Mylonite Zone, which represens the northern part of the Vitis-Pribyslav Fault System, was recognized as important crustal-scale tectonic boundary. It is supposed to have at least partly exhumed the Jihlava Pluton in a dextral transpressive regime around 338-335 Ma (Verner et al., 2006; Žák et al., 2014). Continuing deformation is reported at least till 330-327 Ma (Žák et al., 2011, 2014). The youngest northwest-southeast trending faults (e.g. Jachymov FS) are related to the formation of the Late Pennsylvanian to Permian Central European Basin System and tectonic activity therein (Scheck-Wenderoth et al., 2008). Most of these fault systems were reactivated as brittle faults since the Cretaceous (Brandmayr et al., 1995).

The Freyenstein Fault System is traceable over a distance of some 45 km extending from Windpassing in the south via Freyenstein in the Danube valley to Kleinnondorf in the north (Fig. 1). In its southern part, it is trending northeast-southwest, while towards north it is continuously turning into north-south orientation. In the southernmost part, it cuts through the South Bohemian Batholith, dissecting "fine-grained" granite and WBG (Krenmayr et al., 2006), whereas further in the north it more or less represents the border between the Moldanubian nappes and the South Bohemian Batholith. In the northern part the outcrop situation is very bad, but the Freyenstein Fault System is traceable by the occurrence of quartz-mobilisate and fault rock of the shear zone appearing in a few abandoned quarries and as randomly distributed loose blocks in the countryside. These rocks are shown on Austrian geological map 1:50.000 sheet 35 Königswiesen (Thiele, 1984) and sheet 36 Ottenschlag (Fuchs, 1986) and mentioned in mapping reports of the Geological Survey of Austria (e.g. Fuchs, 1984; Thiele, 1969) as well as in the explanatory notes to the map sheet 36 Ottenschlag (Fuchs and Roetzel, 1990).

3 The Freyenstein Fault System

The description of the shear zone focuses predominantly on a small area located at the section point of the Freyenstein FS and the Danube river close to the village Freyenstein (Fig. 2). This area was chosen, because of the best outcrop situation exposing a more or less complete section across the FS with comparatively fresh rocks. Additionally, spots along less exposed parts were visited, which will be briefly described afterwards. Coordinates of all outcrop and sampling points are given in Table 1.

3.1 Lithologies along the section at the Danube river

Along the Danube river, the Freyenstein FS consists of 300 m thick mylonite. The margin to the country rock is not discrete and represented by c. 100 m protomylonite on both sides, which fluently transits into undeformed granite in the far field. Outcrops mentioned in the text are shown in Fig. 2.

Undeformed granite: Undeformed WBG characteristically appears as roundly exfoliated blocks (Fig. 3a) showing iron hydroxide-discoloration at joint and foliation planes. It is typically light grey and rich in biotite. Up to 7 cm sized, twinned potassium feldspar megacrysts are mostly aligned along an obvious primary magmatic fabric, but occasionally are oriented-randomly (Fig. 3b). They show yellowish colors at their rims due to weathering processes. The WBG is intruded by "fine-grained" granite, which is grey, often shows brownish discoloration and shatters to angular blocks. In few locations, assimilated blocks of WBG occur therein. Younger aplitic granite intrudes both the WBG and the "fine-grained" granite. The contact is discrete, but in some outcrops with complex geometries (Fig. 3c). The aplitic granite shatters to angular blocks, is yellowish and often forms massive bodies. Further, "fine-grained" dioritic dikes occur. Of special interest is the appearance of partly dissolved, slightly foliated and banded lenses of paragneiss in undeformed WBG. They are interpreted as rocks of the Moldanubian nappes incorporated into the intruding granite magma. Localized shear bands dissect this assemblage of otherwise undeformed granitic rocks (outcrop: GG15039).

Protomylonite: At the shear zone margin, beside quartz also feldspar of WBG is "ductily-deformed". The potassium

Sample	Latitude	Longitude	Lithology
GG14007	48°13'08.4"N	14°56'58.4"E	WBG, FGG
GG14008	48°13'02.9"N	14°57'02.5"E	WBG, FGG
GG14009	48°12'57.8"N	14°57'06.5"E	FGG, catacl.
GG14012	48°12'50.9"N	14°57'09.1"E	quartzite, myl.
GG14013	48°12'50.9"N	14°57'08.9"E	FGG, myl.
GG15001	48°12'33.3"N	14°57'17.8"E	WBG
GG15007	48°12'45.1"N	14°57'13.2"E	WBG, myl.
GG15031	48°12'39.0"N	14°57'17.7"E	WBG, ultrac.
GG15039	48°13'17.8"N	14°57'05.2"E	WBG, FGG
GG15040	48°13'10.2"N	14°57'15.2"E	WBG, peg, myl.
GG15041	48°13'02.9"N	14°57'22.6"E	WBG
GG20001	48°21'07.7"N	15°05'50.5"E	Qz-mob, WBG
GG20003	48°29'24.7"N	15°08'30.3"E	Qz-mob
GG20004	48°23'53.7"N	15°07'04.7"E	Qz-mob, WBG
GG20006	48°15'04.6"N	14°59'46.1"E	Qz-mob
GG20009	48°11'12.7"N	14°54'47.4"E	FGG, myl.
15G36	48°12'34.7"N	14°57'18.4"E	WBG
PMM14/09	48°13'20.9"N	14°57'15.1"E	WBG

Table 1: Coordinates (WGS84) of samples and outcrops mentioned in the text. Abbreviations: catacl – cataclastic, FGG – „fine-grained" granite, myl – mylonitic, peg – pegmatite, ultrac – ultracataclastic, WBG – Weinsberg granite, Qz-mob – quartz-mobilisate.

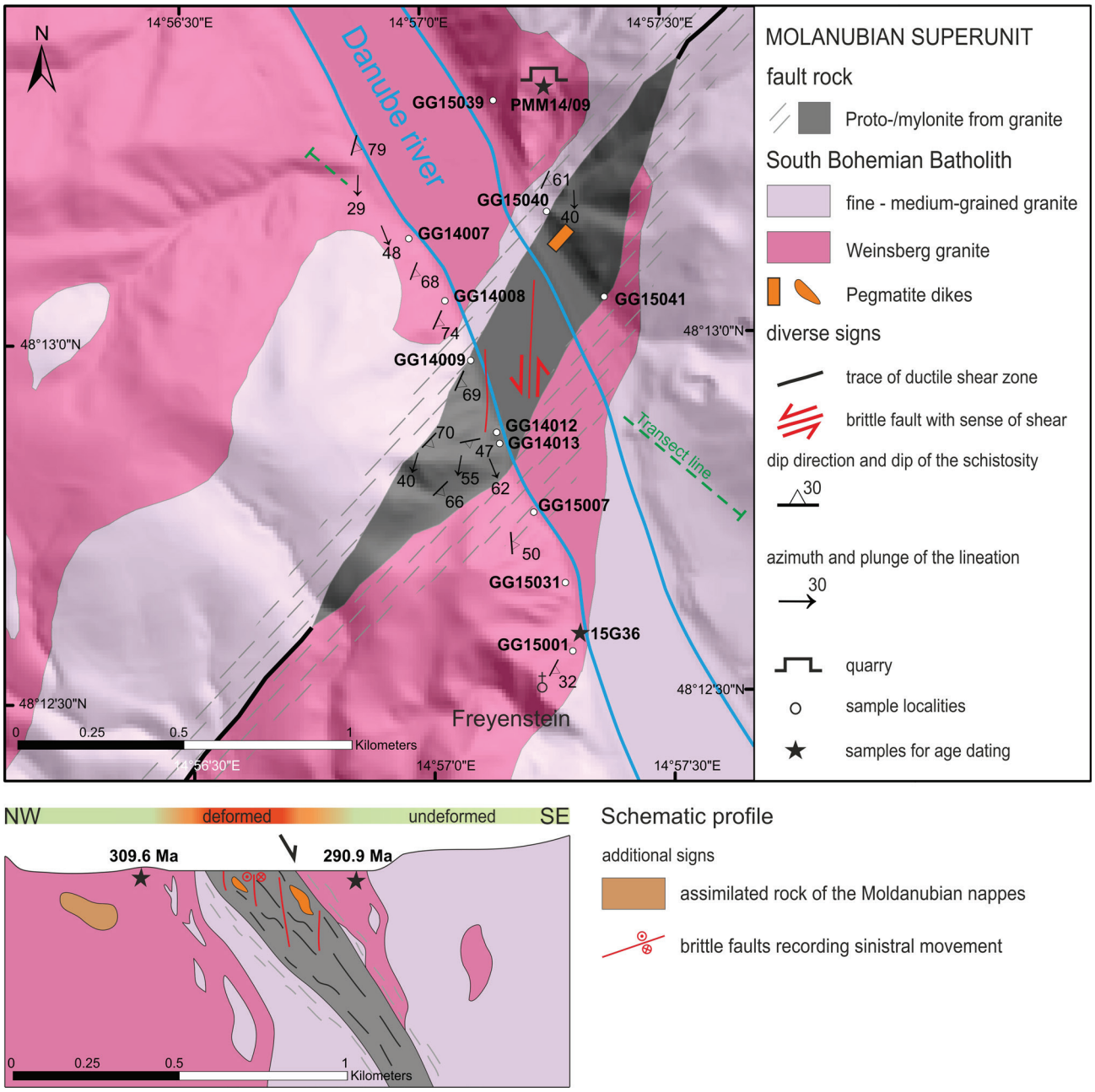

Fig. 2: Map of the investigated area modified after Fuchs (2005) and schematic profile crosscutting the Freyenstein Fault System. Numbers at structures indicate the dipping angle. The transect line is indicated on the map. For legend of the profile see legend of the map, additional signs are complemented. Note that the orientation of the ductile shear zone (black and grey) with normal sense of shear with a dextral component is different from the brittle fault, which is depicted as isolated red lines with sinistral sense of shear. The fault appears only at few locations in the field.

feldspar megacrysts are rounded and grain size is decreasing noticeably to roughly 3 cm (Fig. 3d). Additionally, cohesive ultra-cataclasite occurs. It is usually restricted to small bands of a few centimeter in thickness and appears conspicuously black.

Mylonite: Angularly breaking, light grey, mylonitized orthogneiss, intersected by numerous up to a few centimeter thick feldspar-quartz veins characterizes the core of the shear zone (outcrop: GG14013). One type consists of quartz and feldspar with few muscovite flakes. Diffuse distributed ironoxide/hydroxide causes a yellowish to brownish color. In a second type, more chlorite with remnants of biotite is present. Variable phyllosilicate content causes a gneissic layering (Fig. 3e). „Fine-grained" parts exhibit an ultramylonitic texture and a pervasive SCC´-type shear band fabric (Fig. 3f). A few decimeters thick, "ductily-deformed" pegmatite dikes with up to 1 cm large, slightly kinked muscovite crystals are aligned along the mylonitic foliation (Fig. 3g). This foliation is overprinted partly by brittle deformation, expressed in greenish to "white-colored" quartzite forming slickensides with tearing edges as shear sense indicators (Fig. 3h). Fine- to "medium-grained" quartz rich mylonitized granitic gneiss and aplitic dikes mark the upper boundary to the hangingwall on the northeastern riverside of the Danube (outcrop: GG15041).

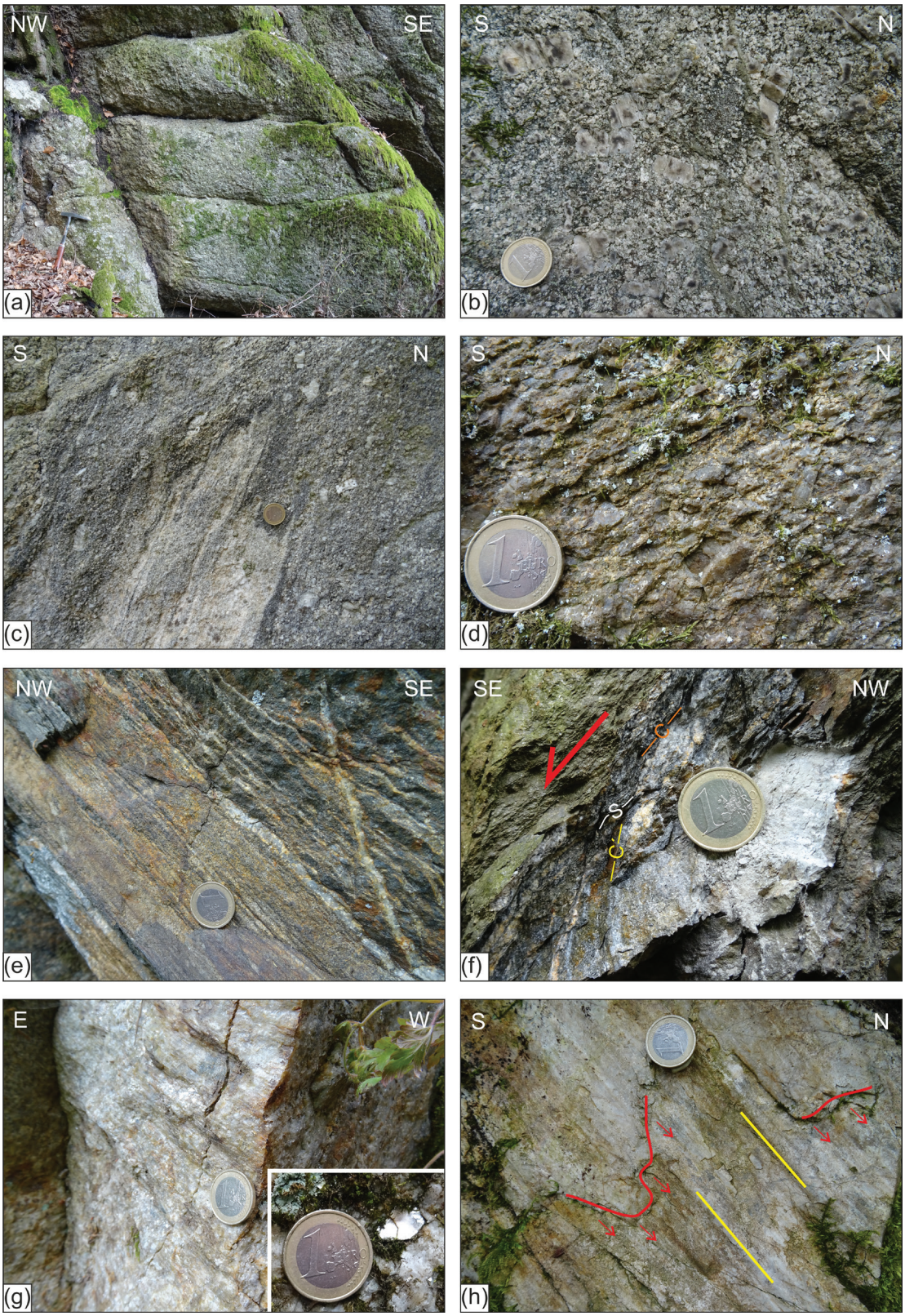

Fig. 3: Examples of undeformed and deformed granite in the investigated area. (a) Weathered blocks of undeformed Weinsberg granite (WBG) (GG15001). (b) Idiomorphic Kfs crystals in undeformed WBG with no preferred orientation embedded in a medium to "coarse-grained" matrix consisting of Qz, Pl and Bt (GG14008). (c) Aplitic dike intruding in WBG granite. The contacts are sharp, indicating that the WBG had already cooled down preventing thus mixing of melts (GG14007). (d) Protomylonitic orthogneiss formed by a WBG protolith. Kfs crystals are rounded and aligned along the schistosity (GG15007). (e) Mylonite near the central part of the shear zone. The layering is due to alternating Qz and Bt rich layers (GG15040). (f) SCC´-type shear band fabric in a mylonite showing top to the south sense of shear (GG15040). (g) "Ductily-deformed" pegmatite dike with Ms crystals up to 1 cm in diameter and brittle slickensides. Inlet: Seldomly, muscovite crystals become larger and are obviously kinked (note the shadow; GG15040). (h) Slickenside in Qz rich, mylonitic orthogneiss. Brittle tearing edges (red) with dip slip indicate north-directed sense of shear. Striations are marked with yellow. Arrows indicate the shearing direction (GG14012). Mineral abbreviations after Whitney and Evans (2010).

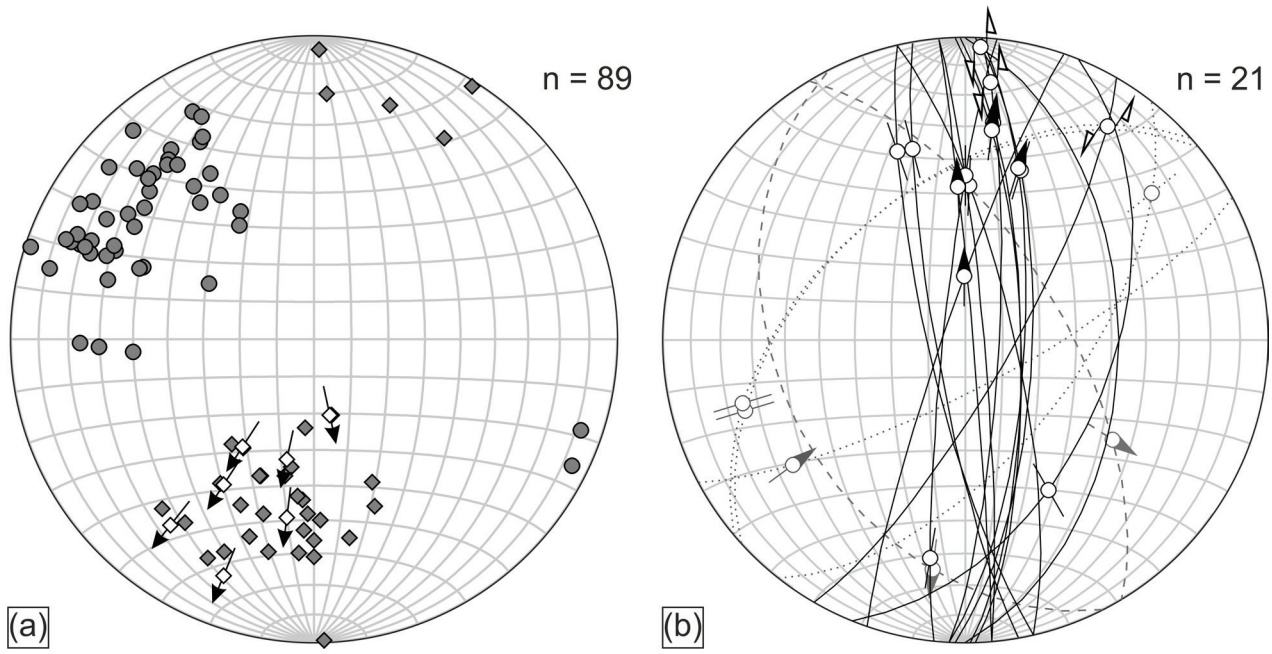

Fig. 4: Equal area lower hemisphere stereoplots. Number of data are indicated (n=X). (a) Stereoplot showing the orientation of the structural elements related to the mylonitic schistosity: Circles represent poles of schistosity planes, whereas the diamonds indicate orientations of stretching lineations. White diamonds with arrow indicate the shear sense. (b) Stereoplot of brittle slickensides and slickenlines thereon. The slickensides are dipping steeply to the east and west (white dots with bars and arrows). The slickenlines are trending north-south with two identified generations: A first one plunging to the north with about 40° and a second shallower plunging one. A set of conjugated fractures is oriented notheast-southwest (dotted lines) and northwest-southeast (dashed lines). Arrows indicate sense of shear.

3.2 Geological structures, petrography and microstructures at the Danube river

The Freyenstein FS strikes northeast-southwest and the mylonitic schistosity is dipping to the southeast with dip angles ranging from 40° to 90°. Mylonitic stretching lineation is trending north(east)-south(west) and plunges with moderate angles from 30° to 70° to the south/southwest (Fig. 4a). Clast geometries and SCC´-type shear band fabrics show top to the south/southwest sense of shear (Fig. 3f).

The shear zone was overprinted by a brittle north-south trending fault, which can only be seen in few locations (see also Fig. 2). The main fault planes dip at steep angles to the east and west. A striation lineation plunges to the north with flat angles from 15° to 40°. Sinistral sense of shear with a small component of northward normal faulting was obtained from shear sense indicators such as tearing edges of slickenside striations and Riedel shears. Additionally, conjugated northeast-southwest and northwest-southeast trending fault patterns with plunge angles around 40° developed that lack clear information for kinematics (Fig. 4b). In some cases, the reactivation of a prior schistosity is observed. Petrographic and microstructural analysis were obtained using the polarized microscope.

Undeformed granite: The WBG shows a magmatic mineral assemblage of Qz, Pl, Kfs and Bt. Accessories like Zrn, Mnz, Ap and Ep occur rarely (mineral abbreviations after Whitney and Evans, 2010). Iron and titanium rich biotite is often aligned along a preferred orientation and slightly chloritized. Potassium feldspar crystals show high temperature characteristics like microclinisation, zoning and twinning (Fig. 5a, b). Additionally, numerous less than 1 mm sized symplectites were found at rims of feldspar crystals.

Protomylonite: Close to the shear zone, feldspar crystals are broken, show rounded edges and quartz crystals are deformed ductily. Locally, the formation of microscale shear bands with grain size reduction is observed at grain boundaries of potassium feldspar or along aligned biotite (Fig. 3f, 5d). During ongoing deformation, mostly at the shear zone margin, a schistosity develops due to aligned biotite and opaque minerals connected with continuing grain size reduction and newly formed muscovite crystals. Chloritization of biotite as well as sericitization of feldspar is eminent, the latter being brittle deformed. Quartz often shows undulous extinction and features compatible with subgrain rotation recrystallization microstructures (Stipp et al., 2002; Jeřábek et al., 2007) and bulging. In the vicinity of the mylonitic core of the shear zone, shape preferred orientation and elongated grains are observed (Fig. 5c-d).

Mylonite: The mylonite is characterized by the mineral assemblage Qz, Fsp, Ms (Ser), Chl and ironoxide/hydroxide. Within the mylonitic foliation, some feldspar porphyroclasts showing microcracks, bent twins and bulging are present (Fig. 5e, f). In the „fine-grained" matrix, quartz dominantly forms elongated grains with subgrain rotation and bulging at the rims. Plagioclase is mostly rounded and inclusion rich. Potassium feldspar is affected by sericitisation, even leading to complete sericite pseudomorphs (Fig. 5g). Muscovite and biotite are partly

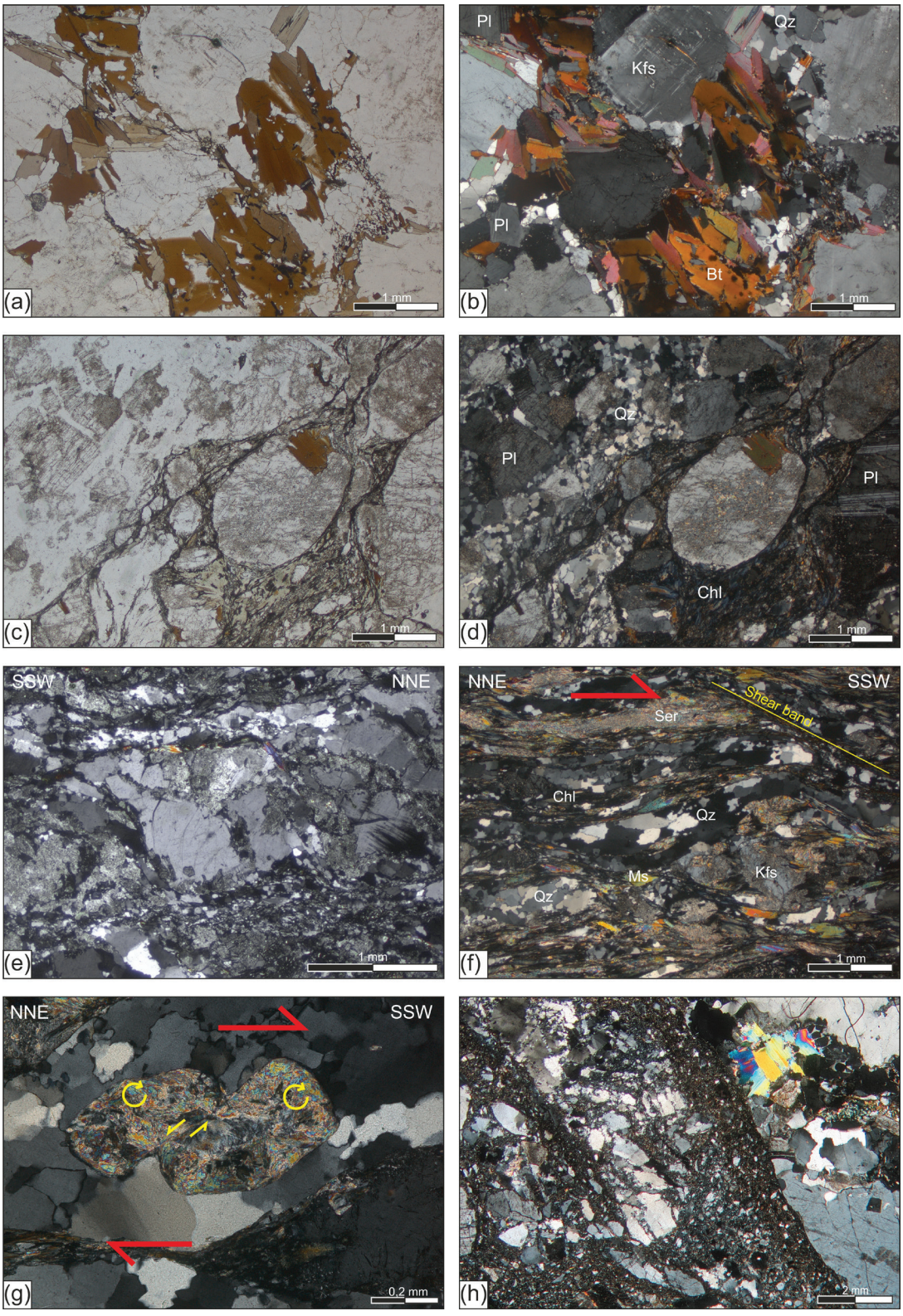

Fig. 5: Photographs of thinsections (thickness c. 25µm) from undeformed granite as well as granite deformed by the Freyenstein Shear Zone: (a) and (b) (GG14007; (b) crossed polarized light - cpl): Undeformed Weinsberg granite. Bt is locally metamict (radioactive halos) and unoriented, Kfs is twinned and shows perthitic exolutions, Pl is characterized by polysynthetic twinning and Qz crystals border at triple junctions. (c) and (d) (GG14009; (d) cpl): Cataclastic orthogneiss. Fsp crystals are rounded at the edges and broken due to deformation (Pl left in picture (c), (d)). Kfs is slightly sericitized. Bt along shear bands is chloritized during (lower) greenschist-facies metamorphic conditions. Cracks are annealed by ironoxides/hydroxides. (e) (GG14012; cpl): Recrystallized Kfs porphyroclast from the core of the shear zone. Note also the sericitisation of Kfs and partly healed twins of Pl on the right side of the picture. (f) (GG15040; cpl): Mylonitic orthogneiss. Clasts of Fsp, which were rather completely sericitized, indicate Weinsberg granite as protolith. Dark layers of chloritized Bt,„fine-grained" Ms, Ser, opaque minerals and Fsp are alternately interlayered with bright layers of Qz, Ms and rare Fsp. Shear bands and clast geometries indicate top to the southsouthwest sense of shear. (g) (PMM14/09; cpl): Sericite pseudomorph after Fsp in a mylonitic orthogneiss. Antithetic slipping with tilted domino boudins indicates a shear sense top to the southsouthwest. (h) (GG15031; cpl): Ultracataclasite mostly consisting of grinded Fsp crystals. A sharp boundary to less destroyed crystals outside the grinding zone is observable. Mineral abbreviations after Whitney and Evans (2010).

undulous and biotite is completely chloritized or dissipated. Several shear sense indicators, like SCC`-type shear band fabrics, mica fishes, asymmetric boudins and clast geometries constrain top to the south/southwest sense of shear (Fig. 5f-g). Seldom, ultracataclasite forming distinct shear bands with sharp boundaries to undestroyed crystals can be observed (Fig. 5h).

3.3 Field observations from badly exposed areas

From the badly exposed areas, several spots are described form north to south. They are depicted in Figure 1 marked by green arrows with numbers (1-6). Pictures taken at these spots are shown in Figure 6 and locations are listed in Table 1.

(1) At the northernmost part of the FS, numerous gravels of quartz-mobilisate can be found randomly distributed at the surface and in the soil (Fig. 6a). They are indicative for the shear zone as no such rocks are present in the undeformed granite of the South Bohemian Batholith in this area as well as in the adjoining paragneiss of the Ostrong Nappe System (Table 1: GG20003). (2) At a small unused quarry to the south, also quartz-mobilisate occurs. The rock is white, rather intransparent and "heavily-jointed" and faulted (Fig. 6b). Nearby, weathered WBG showing a shear band is exposed (Fig. 6c), which might be linked to activity along the Freyenstein FS (Table 1: GG20004). (3) In another abandoned quarry near Gutenbrunn, deformed WBG and pegmatite with a schistosity dipping moderately to the southeast can be observed. Additionally, quartz-mobilisate rock (Fig. 6e), which is heavily jointed and faulted, appears. Unfortunately, no structural data are available from this outcrop as there was no access to the quarry (Table 1: GG20001). (4) At the Kleine Ysper river, again quartz-mobilisate can be found, which is more translucent than the previously described one. Small, minor mylonitized quartz bands can be observed (Table 1: GG20006). (5) In a quarry at the northern side of the Danube river (Table 1: PMM14/09), more than 200 m outside of the mylonitic core of the shear zone, undeformed granite with cracks and some shear bands occurs (Fig. 6d). (6) South of the Danube river near Windpassing, mylonitized „fine-grained" granite is exposed. It is light grey and quartz as well as feldspar are dynamically recrystallized. On a mylonitic schistosity dipping moderately to the southeast, a stretching lineation, which trends north-south, is present. Numerous shear sense indicators like clast geometries, SCC`-type shear band fabrics show top to the south/south-southwest kinematics (Fig. 6g; Table 1: GG20009).

4 Rb-Sr biotite dating

In order to constrain a maximum age for the shear zone deformation, Rb-Sr dating was performed on two samples of nearly undeformed, "coarse-grained" WBG from both sides of the Freyenstein FS. Sample PMM14/09, characterized by biotite with an average grain size of < 2 mm, was taken in a quarry in the footwall of the Freyenstein FS, whereas sample 15G36 taken from the hanging wall contains biotite with about 3 mm in diameter (Fig. 2).

Biotite was separated from sieve fraction 0.2-0.3 mm after crushing of the samples by using a shaking table and a magnetic separator. For purification, the crystals were grinded in alcohol in an agate mortar and dried in acetone. Samples used for dissolution weighed about 100 mg for whole rock powder and c. 200 mg for biotite. Chemical preparation was performed at the Geological Survey of Austria and follows the procedure described by Sölva et al. (2005). Element concentrations were determined by isotope dilution using mixed $^{84}Rb/^{87}Sr$ spikes. Total procedural blanks are ≤ 1 ng for Rb and Sr. Isotopic ratios were measured at the Department of Lithospheric Research, University of Vienna with a ThermoFinnigan® Triton TI TIMS. Sr was run from Re double filaments, whereas Rb was evaporated from a Ta single filament. During measuring, the NBS987 standard yielded a ratio of $^{86}Sr/^{87}Sr = 0.710283 \pm 0.000003$ (n=9, 2σm). Errors of 1% were determined for the $^{87}Rb/^{86}Sr$ ratio based on interactive sample analysis and spike recalibration. Ages were calculated with the software ISOPLOT/Ex (Ludwig, 2003) using the Rb-decay constants of 1.42×10^{-11} year^{-1}.

The measured Rb-Sr data are presented in Table 2 and Figure 7. Rb and Sr contents as well as the $^{87}Rb/^{86}Sr$ and $^{87}Sr/^{86}Sr$ ratios of the investigated samples of WBG are in the range of published data by Scharbert (1987). Sample PMM14/09 fits to the group with high Rb/Sr ratios, whereas the other shows similar Rb/Sr ratios as the group with lower and less variable Rb/Sr ratios as defined in the before mentioned publication. Both biotite concentrates are characterized by high Rb (820-1540 ppm) and low Sr (2.2-3.8 ppm) contents, causing very high $^{87}Rb/^{86}Sr$ ratios of > 2000. The high $^{87}Sr/^{86}Sr$ ratios (> 9.5) indicate a very low initial Sr content, typical for magmatic biotite. Due to these characteristics, the influence of the whole rock on the calculated biotite ages is minor. The calculated ages are 309.6 ± 3.0 (sample PMM14/09) and 290.9 ± 2.9 Ma (sample 15G36). Although the low initial Sr content indicates that the biotites are magmatic, we interpret these ages as cooling ages of the granite through roughly the

Sample	Material	Rb [ppm]	Sr [ppm]	$^{87}Rb/^{86}Sr$	$^{87}Sr/^{86}Sr$	$\pm 2s_m$	Age [Ma]
15G36	WR	333.9	95.31	10.186	0.754283	0.000004	
15G36	Bt	1536	3.739	2292.1	10.19943	0.000336	290.9 ± 2.9
PMM14/09	WR	222.6	275.1	2.3444	0.720215	0.000005	
PMM14/09	Bt	822.4	2.218	1996.9	9.509302	0.000308	309.6 ± 3.0

Table 2: Rb-Sr isotopic data on whole rocks (WR) and biotites from the Weinsberg granite near the Freyenstein FS. Analytical techniques are described in text (section 4), ages are calculated from biotites and WR, assuming an error of ±1% on the determined $^{87}Rb/^{86}Sr$ ratio.

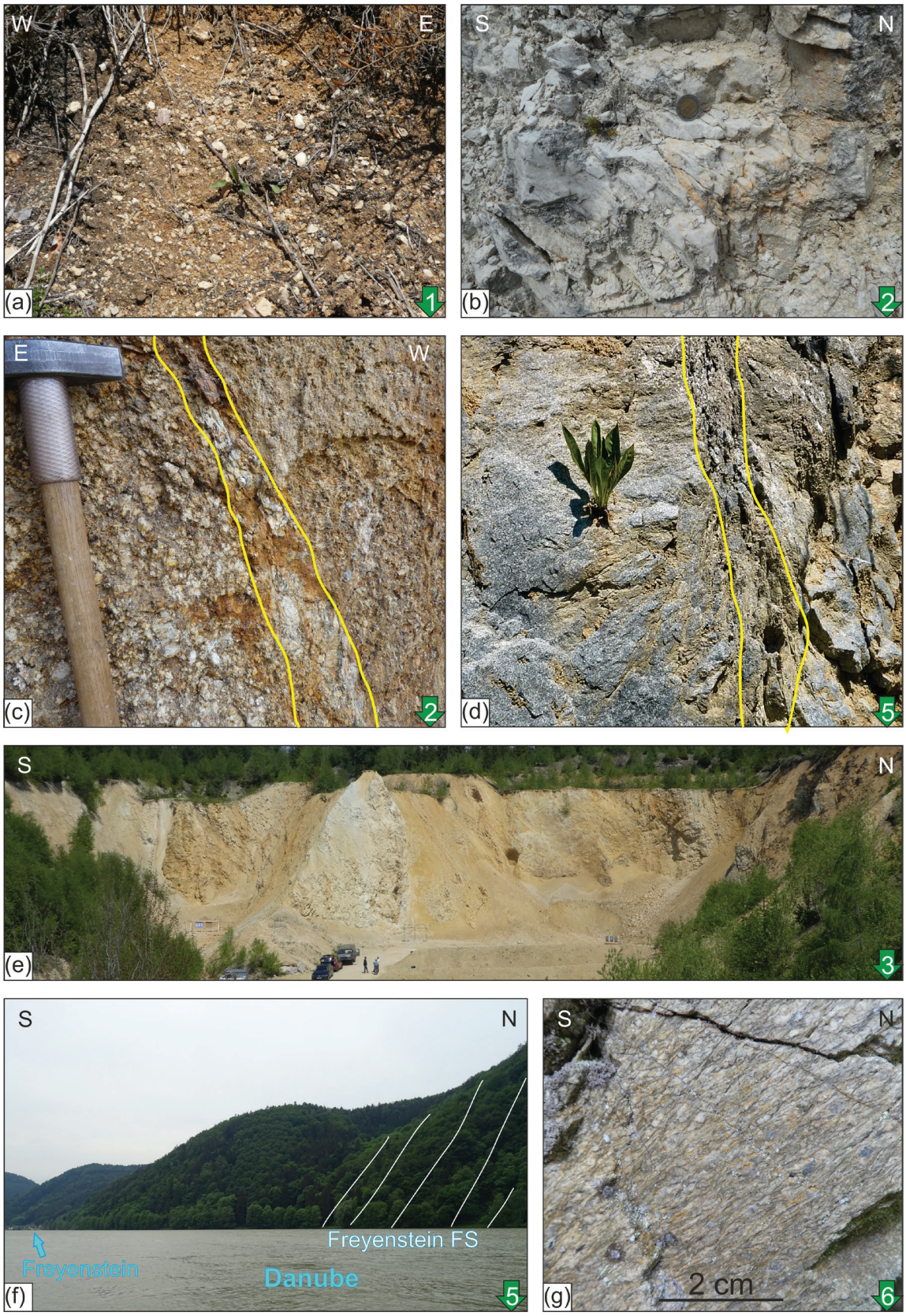

Fig. 6: Impressions of the Freyenstein FS. Green arrows in the right lower corner refer to green arrows in Figure 1. (a) Quartz-mobilisate pebbles close to Kleinnondorf. They are associated with the Freyenstein FS (GG20003). (b) Jointed and broken Quartz-mobilisate in the northern part of the FS (GG20004). (c) Heavily weathered WBG contains a shear band (inside the yellow lines), which roughly follows the orientation of the Freyenstein FS (GG20004). (d) Shear band (inside the yellow lines) in WBG from the quarry near the village Freyenstein (Fig. 2). Image across the Danube river showing the Freyenstein FS was photographed near this spot (see Fig. 6f). (e) Roughly 100 m thick fault rock with quartz-mobilisate along the Freyenstein FS in the quarry near Gutenbrunn (GG20001). (f) View to the west across the Danube river showing the width of the Freyenstein FS (marked with white lines) and the village Freyenstein. (g) Mylonite in the southernmost part near Windpassing. Clast geometries show top to the south (left) sense of shear (GG20009).

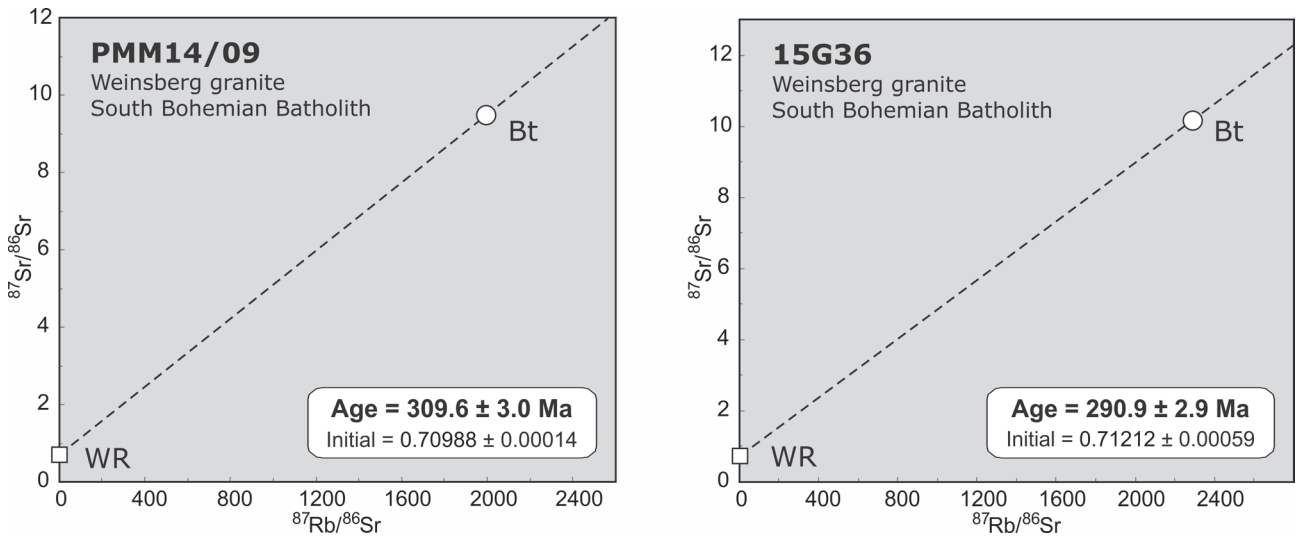

Fig. 7: Rb-Sr biotite ages calculated with the corresponding whole rock (WR) of Weinsberg granite from the southeastern part of the South Bohemian Batholith near the Freyenstein FS. Initial $^{87}Sr/^{86}Sr$ values are related to the calculated ages. The older age (sample PMM14/09) was measured in the footwall, the biotites being c. 3 mm and the younger age (sample 15G36) comes from the hanging wall, the biotites being < 2 mm sized.

300°C isotherm as this is well established that biotites re-equilibrated down to this temperature (Jäger et al., 1967; Thöni, 1996).

5 Discussion

Even though the structure described in this contribution is known for a long time, it was hitherto nameless. However, for handling in GIS related data bases a unique concept including a regional name (type locality) and a hierarchic rank is needed. The structure is perfectly exposed in the area of the village and ruin Freyenstein in the Danube valley (Fig. 2). It includes ductile (shear zone) and brittle (fault) displacement structures which, according to the hierarchic nomenclature of tectonic boundaries proposed by Hintersberger et al. (2017), causes an attribution as a Subfault System or higher ranked Fault System. Considering these aspects, we propose the name Freyenstein Fault System. In its northern part, mainly brittle structures are exposed, whereas in the south additionally "ductily-deformed" rock occurs. Based on our observations, we assume the exposure of different crustal levels along strike.

In the following, the timing of the structure is discussed with respect to its relations to the granitic country rock and metamorphic history of the Moldanubian Superunit. The geologic significance and kinematic relation to other late Variscan fault systems is highlighted.

5.1 Prekinematic or synkinematic granite emplacement?

In the map of Krenmayr et al. (2006), „fine-grained" granite appears predominantly along regional fault systems including the Freyenstein FS. As discussed by Brown (1994) and Petford et al. (2000), shear zones may be active during ascent of melts and the emplacement of magmatic bodies. The question arises, if there is a genetic relation of the „fine-grained" granite to the activity along the investigated shear zone.

Based on field observations, the contact between the WBG and intruded „fine-grained" granite is distinct without any indications for melt mixing. Therefore, emplacement and solidification of the WBG before intrusion of „fine-grained" granite is assumed. Both granite types are affected by the Freyenstein Shear Zone, whereby deformation occurred at a maximum of upper greenschist-facies conditions. This is indicated by the observed deformation features of feldspar with micocracks and bulging, which is typical for temperatures around 450-500°C (Fig. 5e, f; Passchier and Trouw, 2005). As this temperature is clearly below the solidus of granite, a synkinematic intrusion is rather unlikely. Observed microstructural and petrological observations suggest deformation at different temperature. Quartz shows subgrain rotation overprinted by bulging indicating upper greenschist-facies conditions overprinted by lower temperatures (e.g. Stipp et al., 2002). The large amount of chloritized biotite indicates lower greenschist-facies conditions < 350°C (Morad et al., 2011). It is assumed that the Freyenstein Shear Zone was active after the emplacement of the magmatic rocks and during regional cooling.

5.2 Time constraints for activity of the Freyenstein Fault System

Because we could not directly date the deformation in the Freyenstein FS, we try to give age limits for both the ductile and brittle deformation based on data from the literature and "newly-obtained" Rb-Sr biotite cooling ages from the surrounding of the FS.

Constraints for the lower time limit of the ductile deformation can be inferred from Rb-Sr biotite cooling ages as the blocking temperature of biotite represents more or less the lower temperature boundary of ductile deformation in quartz rich lithologies. Unfortunately, within the shear zone biotite is mostly replaced by chlorite. Therefore, Rb-Sr biotite ages were determined from the

adjacent WBG assuming limited frictional heating in the shear zone and thermal equilibrium with the undeformed country rock. These biotite cooling ages from the footwall and hanging wall of the shear zone yield two different age values. As the older age of 309.6 ± 3.0 (sample PMM14/09) was measured in the footwall, whereas the younger age of 290.9 ± 2.9 Ma (sample 15G36) comes from the hanging wall, the age difference cannot be explained by normal faulting along the Freyenstein FS. Most probably, the age gap is due to different grain size in combination with slow cooling of the undeformed magmatic biotite crystals. This may cause a different "effective closure temperature" in the individual samples within the range of 300 ± 50°C as proposed by Jäger et al. (1967) or Thöni (1996). In fact, the biotite grain-size in sample PMM14/09 yielding the older age value is c. 3 mm, whereas it is < 2 mm in sample 15G36 providing the younger age. However, to prove this interpretation and quantify the proposed grain size effect, additional measurements on biotite with different grain size from the footwall and hanging wall, as well as $^{40}Ar/^{39}Ar$ muscovite and fission track ages on zircon and apatite would be necessary. Taking into account the available data and the uncertainties, a lower time limit for ductile deformation at roughly 300 Ma seems plausible. Conversely, the brittle deformation initiated thereafter.

Assuming an initiation of the Freyenstein FS after solidification and cooling of the WBG and „fine-grained" granite to about 500°C, an upper time constrain is given by published intrusion ages. The latter are between 331-322 Ma for the WBG (Finger and Schubert, 2015 and references therein; Mnz, Zrn, ID-TIMS) and between 322 Ma and 316 Ma for the „fine-grained" granite (Gerdes et al., 2003; Rupp et al., 2011; Mnz, ID-TIMS). However, these age data have not been obtained from rocks of the investigated area and especially those from the „fine-grained" granite are determined on spatially separated bodies. Further, there is no precise information about the cooling history and timing when the granitic rocks had cooled to c. 500°C. For this reason we suggest an upper time limit for the initiation of the ductile deformation around 320 Ma.

5.3 Relationship to other fault systems in the Bohemian Massif

The oldest discrete shear zones in the southern part of the Bohemian Massif postdating internal nappe stacking within the Moldanubian Superunit are the "moderately-dipping" Moldanubian Thrust and the subhorizontal Strudengau Shear Zone. The Moldanubian Thrust is a transpressive structure characterized by top to the north/northeast sense of shear before 325 Ma (Fritz et al., 1996; Štípská et al., 1999).

The Strudengau Shear Zone is spatially close to the Freyenstein Fault System and has been active between 323 Ma and 318 Ma (Zeitlhofer et al., 2013). However, even though the activity might be contemporaneous with the ductile Freyenstein Shear Zone, kinematics and orientation differ. Therefore, no clear relationship can be drawn at the current state of knowledge.

Based on the geological map of Krenmayr et al. (2006), it seems that the Freyenstein FS joins with the northeast-southwest oriented Vitis-Pribyslav FS in the area of Zwettl, however field evidence supporting this assumption lacks due to bad outcrop situation. The Pribyslav Mylonite Zone shows top southeast sense of shear with an upper limit of movement around 335-327 Ma (Žák et al., 2014). This is much earlier than the supposed ductile activity along the Freyenstein Shear Zone. However, because of lacking deformation and cooling ages along this shear zone, a tectonic and genetic relationship between both fault systems cannot be excluded. The brittle Vitis Fault is characterized by sinistral displacement at a maximum temperature of c. 300°C (Brandmayr et al., 1995). This kinematic fit to the brittle deformation along the Freyenstein Fault and support a contemporaneous activity after 300 Ma.

Considering all sinistral northeast-southwest trending shear zones, the Diendorf, Vitis and Freyenstein Faults in the east are characterized by brittle deformation overprints (Wallbrecher et al., 1991; Brandmayr et al., 1995, 1999; Büttner, 2007), whereas the Karlstift and Rodl-Kaplice FS in the west record deformation only at (upper) greenschist-facies conditions. This might be explained in two ways. Firstly, the faults in the west are older and the deformation migrated eastward. Secondly, they are contemporaneous and indicate a deeper level of exhumation and therefore a higher metamorphic grade of fault rock in the west. Both possibilities are in line with the regional cooling trend of the southern Bohemian Massif (Scharbert et al., 1997), but unfortunately this trend is poorly constrained due to a limited amount of cooling ages.

6 Conclusions

The presented structural, petrological and geochronological data allow the following conclusion:

- The investigated structure is northeast-southwest to north-south oriented and extends over c. 45 km within the southeastern part of the Moldanubian Superunit. It has been known as brittle, sinistral strike-slip fault and remained nameless. The presented data indicate that it additionally includes an approximately 500 m wide ductile mylonitic shear zone. Since it is perfectly exposed in the area of the village Freyenstein showing ductile shearing and brittle faulting, we propose the name Freyenstein Fault System.
- The ductile shear zone developed during cooling from upper to lower greenschist-facies conditions based on macroscopic and microscopic structures and mineral assemblages. The mylonitic foliation dips to the southeast and gives evidence for normal shearing top to the south/southsouthwest with a dextral strike-slip component.
- Brittle faulting is observed on north-south trending, subvertical slickensides with tearing edges indicating sinistral strike-slip displacement with a normal fault component.
- The activity of the Freyenstein Fault System can be estimated from intrusion ages of granitic rock and

the brittle-ductile transition around 300°C inferred from Rb-Sr biotite cooling ages. Two ages from undeformed Weinsberg granite with different grain size of biotite yield 310 Ma and 290 Ma, respectively. According to the available data, ductile shearing can be restricted to the timespan of 320-300 Ma, whereas brittle faulting happened afterwards.

Acknowledgements

We thank H. Fritz, C. Hauzenberger, B. Huet and M. Linner for fruitful discussions and scientific input. M. Horschinegg is thanked for the Rb and Sr isotopic measurements. Additionally, we thank four reviewers P. Jeřábek, A. Plunder, F. Chopin and H. Fritz for their constructive comments, which helped to improve the manuscript. Special thanks to the editor K. Stüwe for his very helpful comments and suggestions enabling publication of the manuscript.

References

Brandmayr, M., Dallmeyer, R., Handler, R., Wallbrecher, E., 1995. Conjugate shear zones in the Southern Bohemian Massif (Austria): implications for Variscan and Alpine tectonothermal activity. Tectonophysics, 248, 97–116. https://doi.org/10.1016/0040-1951(95)00003-6

Brandmayr, M., Loizenbauer, J., Wallbrecher, E., 1999. Contrasting P-T conditions during conjugate shear zone development in the Southern Bohemian Massif, Austria. Mitteilungen der Österreichischen Geologischen Gesellschaft, 90, 11–29.

Brown, M., 1994. The generation, segregation, ascent and emplacement of granite magma: the migmatite-to-crustally-derived granite connection in thickened orogens. Earth-Science Reviews, 36, 83–130. https://doi.org/10.1016/0012-8252(94)90009-4

Büttner, S.H., 2007. Late Variscan stress-field rotation initiating escape tectonics in the south-western Bohemian Massif: A far field response to late-orogenic extension. Journal of Geosciences, 52, 29–43. https://doi.org/10.3190/jgeosci.004

Cháb, J., Stráník, Z., Eliáš, M., 2007. Geologická mapa České republiky 1:500 000. Česká geologická služba, Praha.

Ertl, A., Schuster, R., Hughes, J.M., Ludwig, T., Meyer, H.-P., Finger, F., Dyar, M.D., Ruschel, K., Rossman, G.R., Klötzli, U., Brandstätter, F., Lengauer, C.L., Tillmanns, E., 2012. Li-bearing tourmalines in Variscan granitic pegmatites from the Moldanubian nappes, Lower Austria. European Journal of Mineralogy, 24, 695–715. https://doi.org/10.1127/0935-1221/2012/0024-2203

Faryad, S.W., 2009. The Kutná Hora Complex (Moldanubian zone, Bohemian Massif): A composite of crustal and mantle rocks subducted to HP/UHP conditions. Lithos, 109, 193–208. https://doi.org/10.1016/j.lithos.2008.03.005

Finger, F. and von Quadt, A., 1992. Wie alt ist der Weinsberger Granit? U/Pb versus Rb/Sr Geochronologie. Mitteilungen der Österreichischen Mineralogischen Gesellschaft, 137, 83–87.

Finger, F., Gerdes, A., Janoušek, V., René, M., Riegler, G., 2007. Resolving the Variscan evolution of the Moldanubian sector of the Bohemian Massif: the significance of the Bavarian and the Moravo-Moldanubian tectonometamorphic phases. Journal of Geosciences, 52, 9–28. https://doi.org/10.3190/jgeosci.005

Finger, F., Gerdes, A., René, M., Riegler, G., 2009. The Saxo-Danubian Granite Belt: magmatic response to post-collisional delamination of mantle lithosphere below the southwestern sector of the Bohemian Massif (Variscan orogen). Geologica Carpathica, 60, 205–212. https://doi.org/10.2478/v10096-009-0014-3

Finger, F. and Schubert, G., 2015. Die Böhmische Masse in Österreich. Was gibt es Neues? Abhandlungen der Geologischen Bundesanstalt, 64, 167–179.

Franke, W., 2000. The mid-European segment of the Variscides: tectonostratigraphic units, terrane boundaries and plate tectonic evolution. Geological Society of London, Special Publications, 179, 35–61.

Friedl, 1997. U/Pb-Datierungen an Zirkonen und Monaziten aus Gesteinen vom österreichischen Anteil der Böhmischen Masse. Dissertation, Universität Salzburg, Österreich. 242pp.

Fritz, H., Dallmeyer, R.D., Neubauer, F., 1996. Thick-skinned versus thin-skinned thrusting: Rheology controlled thrust propagation in the Variscan collisional belt (The southeastern Bohemian Massif, Czech Republic - Austria). Tectonics, 15, 1389–1413. https://doi.org/10.1029/96TC01098

Fuchs, G. and Matura, A., 1976. Zur Geologie des Kristallins der südlichen Böhmischen Masse. Jahrbuch der Geologischen Bundesanstalt, 119, 1–43.

Fuchs, G., 1984. Bericht 1981 über geologische Aufnahmen im Kristallin auf Blatt 36 Ottenschlag. Verhandlungen der Geologischen Bundesanstalt, 1982, 31–33.

Fuchs, G., 1986. Geologische Karte der Republik Österreich Blatt 36 Ottenschlag 1:50.000. Geologische Bundesanstalt, Wien.

Fuchs, G. and Roetzel, R., 1990. Geologische Karte der Republik Österreich 1:50000 Erläuterungen zu Blatt 36 Ottenschlag. Geologische Bundesanstalt. 67 pp.

Fuchs, G., 2005. Der geologische Bau der Böhmischen Masse im Bereich des Strudengaus (Niederösterreich). Jahrbuch der Geologischen Bundesanstalt, 145, 283–291.

Gerdes, A., Friedl, G., Parrish, R.R., Finger, F., 2003. High-resolution geochronology of Variscan granite emplacement the South Bohemian Batholith. Journal of the Czech Geological Society, 48, 53–54.

Hintersberger, E., Iglseder, C., Schuster, R., Huet, B., 2017. The new database "Tectonic Boundaries" at the Geological Survey of Austria. Jahrbuch der Geologischen Bundesanstalt, 157, 195–207.

Jäger, E., Niggli, E., Wenk, E., 1967. Rb/Sr Altersbestimmungen an Glimmern der Zentralalpen. Beiträge zur geologischen Karte der Schweiz, NF 1344, Bern, 67 pp.

Jeřábek, P., Stünitz, H., Heilbronner, R., Lexa, O., Schulmann, K., 2007. Microstructural-deformation record of

an orogen-parallel extension in the Vepor Unit, West Carpathians. Journal of Structural Geology, 29/11, 1722–1743. https://doi.org/10.1016/j.jsg.2007.09.002

Klötzli, U.S. and Parrish, R.R., 1996. Zircon U/Pb and Pb/Pb geochronology of the Rastenberg granodiorite, South Bohemian Massif, Austria. Mineralogy and Petrology, 58, 197–214. https://doi.org/10.1007/BF01172096

Klötzli, U., Frank, W., Scharbert, S., Thöni, M., 1999. Evolution of the SE Bohemian Massif based on Geochronological data - A Review. Jahrbuch der Geologischen Bundesanstalt, 141, 377–394.

Koller, F., Scharbert, S., Höck, V., 1993. Neue Untersuchungen zur Genese einiger Granite des Südböhmischen Plutons. Mitteilungen der Österreichischen Mineralogischen Gesellschaft, 138, 179–196.

Kotková, J., 2007. High-pressure granulites of the Bohemian Massif: recent advances and open questions. Journal of Geosciences, 52, 45–71. https://doi.org/10.3190/jgeosci.006

Krenmayr, H.G., Schnabel, W., Bryda, G., Egger, H., Finger, F., Linner, M., Mandl, G.W., Nowotny, A., Pestal, G., Reitner, J.M., Roetzel, R., Rupp, C., Schuster, R., Van Husen, D., 2006. Geologische Karte von Oberösterreich 1:200.000. Geologische Bundesanstalt, Wien.

Kroner, U. and Romer, R.L., 2013. Two plates - Many subduction zones: The Variscan orogeny reconsidered. Gondwana Research, 24, 298–329. https://doi.org/10.1016/j.gr.2013.03.001

Linner, M., 2013. Metamorphoseentwicklung und Deckenbau des Moldanubikums mit Fokus auf den Raum Melk – Dunkelsteinerwald. In: Gebhardt, H. (eds.) Tagungsband zur Arbeitstagung 2013 der Geologischen Bundesanstalt. Geologie der Kartenblätter 55 Ober-Grafendorf und 56 St. Pölten, Wien, pp. 43–56.

Ludwig, K.R., 2003. Isoplot/Ex version 3.0. A geochronological toolkit for Microsoft Excel. Berkeley Geochronological Centre: Special Publication, 70 pp.

Morad, S., Sirat, M., El-Ghali, M.A.K., Mansurbeg, H., 2011. Chloritization in Proterozoic granite from the Äspö Laboratory, southeastern Sweden: record of hydrothermal alterations and implications for nuclear waste storage. Clay minerals, 46/3, 495-513. https://doi.org/10.1180/claymin.2011.046.3.495

Neubauer, F., Dallmeyer R.D., Fritz, H., 2003. Chronological constraints of late- and post-orogenic emplacement of lamprophyre dykes in the southeastern Bohemian Massif, Austria. Schweizerische Mineralogische und Petrographische Mitteilungen, 83, 317–330.

Passchier, C.W. and Trouw, R.A.J., 2005. Microtectonics. Springer Berlin Heidelberg New York, xi+366 pp.

Perraki, M. and Faryad, S.W., 2014. First finding of microdiamond, coesite and other UHP phases in felsic granulites in the Moldanubian Zone: Implications for deep subduction and a revised geodynamic model for Variscan Orogeny in the Bohemian Massif. Lithos, 202–203, 157–166. https://doi.org/10.1016/j.lithos.2014.05.025

Petford, N., Cruden, A.R., McCaffrey, K.J., Vigneresse, J.L., 2000. Granite magma formation, transport and emplacement in the Earth's crust. Nature, 408, 669–673. https://doi.org/10.1038/35047000

Petrakakis, K., 1997. Evolution of Moldanubian rocks in Austria: review and synthesis. Journal of Metamorphic Geology, 15, 203–222. https://doi.org/10.1111/j.1525-1314.1997.00015.x

Racek, M., Lexa, O., Schulmann, K., Corsini, M., Štípská, P., Maierová, P., 2017. Re-evaluation of polyphase kinematic and 40Ar/39Ar cooling history of Moldanubian hot nappe at the eastern margin of the Bohemian Massif. International Journal of Earth Sciences (Geologische Rundschau) 106, 397–420. https://doi.org/10.1007/s00531-016-1410-4

Rupp, C., Linner, M., Mandl, G.W., 2011. Erläuterungen zur Geologischen Karte von Oberösterreich 1:200.000. Geologische Bundesanstalt, Wien, 255 pp.

Scharbert, S., 1987. Rb-Sr Untersuchungen granitoider Gesteine des Moldanubikums in Österreich. Mitteilungen der Österreichischen Mineralogischen Gesellschaft, 132, 21–37.

Scharbert, S., Breiter, K., Frank, W., 1997. The Cooling History of the Southern Bohemian Massif. Journal of the Czech Geological Society, 42, 24.

Scheck-Wenderoth, M., Krzywiec, P., Zühlke, R., Maystrenko, Y., Froitzheim, N., 2008. Permian to Cretaceous tectonics. In: McCann, T. (eds.) The Geology of Central Europe, Geological Society of London, London, 2: Mesozoic and Cenozoic, pp. 999–1030.

Schantl, P., Hauzenberger, C., Finger, F., Müller, T., Linner, M., 2019. New evidence for the prograde and retrograde PT-path of high-pressure granulites, Moldanubian Zone, Lower Austria, by Zr-in-rutile thermometry and garnet diffusion modelling. Lithos, 342–343, 420–439. https://doi.org/10.1016/j.lithos.2019.05.041

Schnabel, W., Bryda, G., Egger, H., Fuchs, G., Krenmayr, H.G., Mandl, G.W., Matura, A., Nowotny, A., Roetzel, R., Scharbert, S., Wessely, G., 2002. Geologische Karte von Niederösterreich 1:200.000. Geologische Bundesanstalt, Wien.

Siebel, W., Blaha, U., Chen, F., Rohrmüller, J., 2005. Geochronology and geochemistry of a dyke-host rock association and implications for the formation of the Bavarian Pfahl shear zone, Bohemian Massif. International Journal of Earth Sciences (Geologische Rundschau), 94, 8–23. https://doi.org/10.1007/s00531-004-0445-0

Sölva, H., Grasemann, B., Thöni, M., Thiede, R., Habler, G., 2005. The Schneeberg Normal Fault Zone: normal faulting associated with Creaceous SE- directed extrusion in the Eastern Alps (Italy/Austria). Tectonophysics, 401, 143–166. https://doi.org/10.1016/j.tecto.2005.02.005

Sorger, D., Hauzenberger, C.A., Linner, M., Iglseder, C., Finger, F., 2018. Carboniferous polymetamorphism recorded in paragneiss-migmatites from the Bavarian Unit (Moldanubian Superunit, Upper Austria): implications for the tectonothermal evolution at the end of the Variscan orogeny. Journal of Petrology, 59, 1359–1382. https://doi.org/10.1093/petrology/egy063

Sorger, D., Hauzenberger C.A., Finger, F., Linner, M., 2020. Two generations of Variscan garnet: Implications from a petrochronological study of a high-grade Avalonia-derived paragneiss from the Drosendorf unit, Bohemian Massif. Gondwana Research, 85, 124–148. https://doi.org/10.1016/j.gr.2020.04.004

Stipp, M., Stünitz, H., Heilbronner, R., Schmid, S.M., 2002. Dynamic recrystallization of quartz: correlation between natural and experimental conditions. Geological Society of London, Special Publications, 200/1, 171–190.

Štípská, P., Schulmann, K., Höck, V., 1999. Complex metamorphic zonation of the Thaya dome: result of buckling and gravitational collapse of an imbricated nappe sequence. Geological Society of London, Special Publications, 169, 197–211. https://doi.org/10.1144/GSL.SP.2000.169.01.15

Suess, F.E., 1908. Die Beziehungen zwischen dem moldanubischen und dem moravischen Grundgebirge in dem Gebiete von Frain und Geras. Verhandlungen der Geologischen Reichsanstalt, 1908, 393–412.

Suess, F.E., 1911. Die Moravischen Fenster und ihre Beziehung zum Grundgebirge des Hohen Gesenkes. Denkschriften der Kaiserlichen Akademie der Wissenschaften Mathematisch–naturwissenschaftliche Klasse, 88, 541–631.

Thiele, O., 1969. Bericht 1968 über Aufnahmen auf den Blättern Königswiesen (35) und Zwettl (19). Verhandlungen der Geologischen Bundesanstalt, 1969, 75–76.

Thiele, O., 1976. Ein westvergenter kaledonischer Deckenbau im niederösterreichischen Waldviertel? Jahrbuch der Geologischen Bundesanstalt, 119, 75–81.

Thiele, O., 1984. Geologische Karte der Republik Österreich Blatt 35 Königswiesen 1:50.000. Geologische Bundesanstalt, Wien.

Thöni, M., 1996. Isotopengeologie und Geochronologie – Einsatzmöglichkeiten in der Geologie. Mitteilungen der Geologie- und Bergbaustudenten Österreich, 39/40, 187–209.

Tollmann, A., 1982. Großräumiger variszischer Deckenbau im Moldanubikum und neue Gedanken zum Variszikum Europas. Geotektonische Forschungen, 64, 1–91.

Vellmer, C. and Wedepohl, K., 1994. Geochemical characterization and origin of granitoids from the South Bohemian Batholith in Lower Austria. Contributions to Mineralogy and Petrology, 118, 13–32. https://doi.org/10.1007/BF00310608

Verner, K., Žák, J., Hrouda, F., Holub, F.V., 2006. Magma emplacement during exhumation of the lower-to mid-crustal orogenic root: the Jihlava syenitoid pluton, Moldanubian Unit, Bohemian Massif. Journal of Structural Geology, 28/8, 1553–1567. https://doi.org/10.1016/j.jsg.2006.03.037

Waldmann, L., 1930. Aufnahmsbericht des Privatdozenten Dr. Leo Waldmann über Blatt Gmünd – Litschau (4454). Verhandlungen der Geologischen Bundesanstalt, 1930, 38–41.

Wallbrecher, V.E., Dallmeyer, R.D., Brandmayr, M., Handler, R., Maderbacher, F., Platzer, R., 1991. Kinematik und Alter der Blattverschiebungszonen in der südlichen Böhmischen Masse. In: Roetzel, R. (eds.) Tagungsband zur Arbeitstagung 1991 der Geologischen Bundesanstalt. Geologie am Ostrand der Böhmischen Masse in Niederösterreich, Schwerpunkt Blatt 21 Horn, Wien, pp. 35–48.

Wallbrecher, V.E., Brandmayer, M., Loizenbauer, J., Handler R., Dallmeyer., 1996. Konjugierte Scherzonen in der südlichen Böhmischen Masse: variszische und alpidische kinematische Entwicklungen. Exkursionsunterlagen für die Wandertagung 1996: Ein Querschnitt durch die Geologie Oberösterreichs, 12–28.

Whitney, D.L. and Evans, B.W., 2010. Abbreviations for names of rock-forming minerals. American Mineralogist, 95, 185–187. https://doi.org/10.2138/am.2010.3371

Žák, J., Verner, K., Finger, F., Faryad, S.W., Chlupáčová, M., Veselovský, F., 2011. The generation of voluminous S-type granites in the Moldanubian unit, Bohemian Massif, by rapid isothermal exhumation of the metapelitic middle crust. Lithos, 121(1-4), 25-40. https://doi.org/10.1016/j.lithos.2010.10.002

Žák, J., Verner, K., Janoušek, V., František, V., Holub, F.V., Kachlík, V., Finger, F., Hajná, J., Tomek, F., Vondrovic, L., Trubač, J., 2014. A plate-kinematic model for the assembly of the Bohemian Massif constrained by structural relationships around granitoid plutons. Geological Society of London, Special Publications, 405, 169–196. http://dx.doi.org/10.1144/SP405.9

Zeitlhofer, H., Schneider, D., Grasemann, B., Petrakakis, K., Thöni, M., 2013. Polyphase tectonics and late Variscan extension in Austria (Moldanubian Zone, Strudengau area). International Journal of Earth Sciences, 103, 83–102. https://doi.org/10.1007/s00531-013-0952-y

Zeitlhofer, H., Grasemann, B., Petrakakis, K., 2016. Variscan potassic dyke magmatism of durbachitic affinity at the southern end of the Bohemian Massif (Lower Austria). International Journal of Earth Sciences, 105, 1175–1197. https://doi.org/10.1007/s00531-015-1238-3

Received: 23.01.2020
Accepted: 10.09.2020
Editorial handling: Kurt Stüwe